

Conversion of South African clays into high quality zeolites

Nicholas M. Musyoka^{1*}, Roland Missegue², Melissa Kuisikana² and Leslie F. Petrik²

¹*Council for Scientific and Industrial research, P. O Box 395, Pretoria, 0001, South Africa.*

²*Environmental and Nano Science Research Group, Department of Chemistry, University of the Western Cape, Private Bag X17 Bellville, 7535, South Africa.*

**Corresponding author's e-mail: nmusyoka@csir.co.za, Tel: +27 012 841 2128*

Abstract

Clays obtained from South Africa were used as feedstock materials for the synthesis of zeolites. The conventional alkaline hydrothermal treatment of the starting material (90°C for 8 hours) was preceded by a fusion step (550°C for 1.5 hours) to improve the solubility of aluminium and silicon. Various characterization techniques such as X-ray diffraction (XRD), X-ray fluorescence (XRF), scanning electron microscopy (SEM) and Fourier transform infrared spectroscopy (FTIR) were employed to probe the properties of the as-received clays as well as resulting zeolitic phase. The synthesized zeolite X and hydroxy-sodalite was of high crystalline quality hence making clay materials a cheaper alternative for producing high quality zeolites.

1. Introduction

Zeolites form an important group of inorganic materials with variable industrial interest, which is derived from their molecular sieving, ion exchange and catalytic properties (Sharma & Sambhi, 2010). The origin of zeolites can be either natural or synthetic. Zeolite formation in nature requires a few hundred to tens of millions of years depending on the chemical environment (Breck, 1974). Early synthesis of zeolites was carried out by crystallization of sodium aluminosilicate gels prepared from pure sodium aluminate, sodium silicate and sodium hydroxide solutions (Breck, 1974; Donahoe and Liou, 1984; Nagy *et al.*, 1998; Byrappa and Yoshimura, 2001). However the high cost and limited availability associated to these chemicals have prompted researchers to seek alternative low cost raw materials. Some of the alternative unconventional feedstocks are such as; coal fly ash (Musyoka *et al.*, 2013), rice husks (Dalai *et al.*, 1985), natural clay minerals (Ghosh, 1994; Chaudhuri *et al.*, 2002; Sharma and Sambhi, 2010; Belviso *et al.*, 2013) and bagasse (Moisés *et al.*, 2013), among other feedstocks. The type and source of silica and alumina feedstock strongly influences the quality and the purity of the final zeolite product (Coombs *et al.*, 1959).

Clays are phyllosilicate minerals which form a layered structure, whereas zeolites form a rigid three dimensional structure with interconnected tunnels and cages (Guggenheim, 1995; Weitkamp and Puppe, 1999). There are three procedures of clay formation which are erosion, diagenesis and weathering (Blatt, 1980; Tazaki *et al.*, 1989). Some attempts have been carried out on the synthesis of clay minerals in the laboratory (Kloprogge *et al.*, 1999). Clays possess plasticity when exposed to water and harden when dried and are composed mainly of grained

minerals that make up colloid fraction of particle size of about 2 μm (Guggenheim, 1995). Since natural clays are an economically attractive source of Si and Al (Basaldella, et al. 1997; Mignoni et al., 2007), the use of these materials would provide an alternative feedstock for the synthesis of high quality zeolites. Sharma and Sambhi (2010) synthesised zeolite Na-A from low-grade Indian clays and reported that the conversion of clays to zeolites depends on the origin and physicochemical properties of the clays. Ghosh *et al.* (1994) converted calcined diatomaceous clay to zeolite A by the hydrothermal method.

This study aimed to implement the hydrothermal conversion of clays that are found in South Africa namely bentonite, white clay and red clay to zeolites. The red low-grade clay is obtained from old brickyards. The wide availability of clay minerals in South Africa and their composition makes them candidates to compete with other silica and alumina feedstocks for the synthesis of high value zeolites. The conventional two-step alkaline hydrothermal treatment of the starting material was preceded by a fusion step to improve the solubility of aluminium and silicon.

2. Experimental

2.1 Materials

Bentonite was obtained from Ecca Holdings Mine Company, white clay was purchased from CRAMMIX and red clay comes from an old brickyard in Barrydale, Western Cape province of South Africa. NaOH pearls and $\text{Al}(\text{OH})_3$ were purchased from KIMIX.

2.2 Synthesis Procedure

50 g clay material (bentonite, white clay or red clay) was thoroughly mixed with 60 g NaOH pearls in a 1:1.2 mass ratio to obtain a homogeneous mixture. Then the mixture was heated in a porcelain crucible at 550°C for 1½ hr. The fused product was laurel-green. Afterwards, the fused material was grounded to powder and was used to synthesize zeolites in two different ways: In the first instance, 20 g of the powdery fused clay was mixed with 100 mL deionised water in a 250 mL bottle. In the other experimental run, 20 g of the powdery fused clay was mixed with 100mL deionised water in a 250 mL bottle, 1.2 g Al(OH)₃ was supplemented to the solution. In both cases the mixture was independently aged in a sealed plastic bottle at room temperature under stirring condition for a set period of 30 min. The molar regimes of the resulting unseparated fused clay slurries is as shown in Table 1, no water loss occurred as the mixture was in a sealed container during stirring. The formed gel slurry was put in the oven for 8 hr of hydrothermal crystallization at a desired temperature of 90°C. Thereafter the resulting solid product was separated from the supernatant and repeatedly washed using deionised water prior to filtration by centrifugal action. The solid product was then dried in the oven at 90°C for 12 hours. The dried product was grounded and labelled accordingly for analysis.

2.3 Characterization

X-ray diffraction (XRD) analysis of the feedstock (clays) and zeolitic products was performed using a Philips X-ray diffractometer. The phase identification was conducted by searching and matching the obtained spectra with the powder diffraction file data base. Major elemental

analysis, expressed in oxide form, was carried out by X-ray fluorescence (XRF) analysis using Philips PW 1480 X-ray fluorescence spectrometer. The spectrometer was fitted with a chromium tube, five analysing crystals namely LIF 200, LIF 220, GE, PE and PX 65 and the detectors are a combination gas-flow proportional counter and a scintillation detector. The gas-flow proportional counter uses P10 gas, which is a mixture of argon and methane at 9:1 ratio. Hitachi X-650 scanning electron microanalyser was used for morphological analysis. In this case the samples were mounted on aluminum studs and coated with a thin film of gold to make them conductive. Fourier transform infrared spectroscopy (FTIR) was used to monitor structural changes that took place during the conversion of clays to zeolites. Approximately 15 mg of each sample was placed on the attenuated total reflectance (ATR) sample holder of a Perkin Elmer spectrum 100 FT-IR spectrometer. Vibrations common to zeolites and clays were identified.

3. Results and discussion

The main elemental composition of the clay materials were analysed and the results are presented in Table 2. Bentonite, white and red clays were found to have the $\text{SiO}_2/\text{Al}_2\text{O}_3$ ratios of 4.58, 4.59 and 3.86, respectively. The $\text{SiO}_2/\text{Al}_2\text{O}_3$ ratio of the feedstock is of paramount importance since it governs the type and framework of zeolite to be synthesized. Therefore these ratios make them suitable starting materials for the synthesis of high value zeolites. All the three clays were also found to contain oxides of exchangeable cations such as Ca, Mg, Fe, Na and K with percentage varying depending on the type of clay. The red clay was observed to have a relatively higher content of Fe and K. White clay contained lesser Ca, Fe, Mg and Na but with the highest Si content. Depending on the type of application for the clay material, these cations can be exchanged to other desirable cations. For example, replacements of uni- and divalent

cations by other di-, tri- or tetravalent cations in the interlayer space of clays enables them to be used as catalysts in the chemical industry (Konta *et al.*, 1995). Another factor that was investigated was the addition of $\text{Al}(\text{OH})_3$ to adjust the $\text{SiO}_2/\text{Al}_2\text{O}_3$ ratio in the fused clay slurry. As had been shown in Table 1, that the addition of $\text{Al}(\text{OH})_3$ changed the molar regime of unseparated fused clay slurries. This should affect the type and quality of the synthesized zeolites.

Mineralogical and morphological analyses presented in Figure 1 shows that the three clays have a layered crystalline structure. This observation was also in agreement to studies by Ralph (1968), Guggenheim (1995) and Belviso *et al.*, (2013). Bentonite was mainly composed of montmorillonite, muscovite, quartz and clinoptilolite mineral phases. As highlighted by Murray *et al* (2000), bentonites are mainly comprised of smectite minerals which are demonstrated by the presence of montmorillonite in the bentonite used in this study. The white and red clays had three common minerals which were kaolinite, quartz and muscovite. This mineralogical composition made them to be classified in the kaolin group of clays. The reason for the commonality of quartz, among other mineral phases, is attributed to the fact that clay minerals are formed by gradual chemical weathering of silicate bearing rocks. The scanning electron micrographs of the three clays revealed that they all contained irregular platelets; poorly defined flakes that contained sub-rounded particles for the bentonite and white clay whereas red clay had cubic-like, ragged-edged particles. The particle size fractions were observed to be between 2 and 10 μm . The particle size, shape, and distribution have been reported to be a very important property in determining the industrial uses of clays (Murray, 2000).

From the spectral data presented in Figure 2, it can be noted that all three clay samples had almost similar vibrational bands. The bands appearing at around 800 cm^{-1} can be associated with Al-O or Si-O symmetric stretching vibrations that correspond to quartz. Analyses done by Colthup *et al.*, (1964) have suggested that the band at 1156 cm^{-1} is most likely to be from the asymmetrical stretching vibration and symmetrical vibration of the Al-O-Si groups, respectively. Vibrational bands between 1000 and 1032 cm^{-1} have been reported to be attributed to Si-O stretching. The silicate bands are often reported to be broad and diffuse because of the overlapping character of different types of silicate molecular vibrations that result from the various silicate minerals (Mollah *et al.*, 1999). In particular case, bentonite had a vibrational band at 632 cm^{-1} that distinguishes it from the other materials, which was assigned to Al-O deformation. White and red clays were also noted to have an extra band at 697 and 698 cm^{-1} respectively and it was attributed to coupled Al-O and Si-O.

Figure 3 and 4 compared the mineralogy of the resulting synthesis product obtained with and without the addition of extra Al in the synthesis mixture. As observed from the X-ray diffraction patterns presented in Figure 3, for the synthesis conducted without the addition of the extra Al to the clay synthesis mixture, a mixture of hydroxy-sodalite zeolite and zeolite X was formed when starting from bentonite and red clay whereas the main zeolitic product formed from white clays was hydroxy-sodalite zeolite. The relatively low intensity ‘hump’ in the XRD diffraction pattern appearing between $20 - 40^\circ 2\theta$, for bentonite and white clay-derived zeolite, can be associated with the presence of an amorphous material which means that complete zeolitization of the clay material had not occurred. Upon addition of extra Al to the synthesis mixture (Figure 4), zeolite

X was found to be the main zeolitic material that was formed after the hydrothermal crystallization. A well-defined morphology for the formed zeolite X was observed when starting from red clay synthesis feedstock. Comparing the obtained zeolite X with that reported in other studies (Pfenninger, 1999), the clay-derived zeolite X had almost the same mineralogical and morphological properties. Zeolite X has numerous industrial applications such as in catalysis, purification and separation of gases and organic components, cation exchange and adsorption (Nagy *et al.*, 1998; Byrappa and Yoshimura, 2001). Due to these wide applications, this zeolite type has become an important target for synthesis from many unconventional starting materials such as rice husk ash, metakaolin, oil shale ash, coal fly ash among other Si-Al containing feedstocks.

During zeolite synthesis subtle changes in the preparation conditions as well as in chemical composition is known to influence the type of zeolite phase that crystallizes from the synthesis mixture (Martínez and Pérez-Pariente, 2011). Clays used in this study were found to have a relatively lower Al content compared to their Si content (Table 2), therefore the addition of the extra Al served to adjusting their Si/Al ratio. Sodalite is the only known zeolitic phase that crystallizes in the full compositional range of Si/Al i.e from 1 to ∞ (Barrer, 1982). A study by Basaldella, et al. (1997) reported that aluminium concentration in the synthesis mixture not only influences the nucleation rate but also the size and morphology of the zeolite crystals. In this study, the modification of the aluminium concentration, without changing the total time of the process of synthesis, was found to influence the type of zeolite formed (Figure 4). Since the mechanism of zeolite formation is a very complex process (Byrappa and Yoshimura, 2001), the change in the quantity of Al in the reaction mixture was expected to influence the silicate and

aluminosilicates polyanion chemistry which could also determine the properties of the resulting material, such as the zeolites' structure, Si and Al distribution in the lattice, morphology, crystal sizes, among other properties (Nagy *et al.*, 1998).

From the infrared spectra in Figure 5, it can be noted that the resulting zeolitic material (both hydroxyl-sodalite and zeolite X) had almost similar characteristic bonds as those found in the clay feedstock. Of the main similarity, vibration bands appearing around 1000 cm^{-1} and between 750 and 400 cm^{-1} are attributed to the characteristic behaviour of aluminosilicates containing materials (Schroeder, 2002; Musyoka *et al.*, 2013). The shift noted in the vibrational band appearing between 810 and 1200 cm^{-1} , when comparing the spectra for zeolites synthesized with (967 cm^{-1}) and without additional Al (980 cm^{-1}), can be attributed to the effect of the extra Al in the synthesis matrix which is a good reflection of the different zeolitic phases that were produced. It is important to monitor these structural changes that take place during the conversion of clays to zeolites since it serves to complement other characterization techniques and can also be used to pick out some elusive anomalies.

4. Conclusion

The results in this study have shown that different zeolites can be prepared starting from different South African clays. In this case, a nearly pure phase of hydroxysodalite and zeolite X was produced with and without additional Al in the synthesis mixture, respectively. The study further demonstrates that with the right control of synthesis conditions, clays sourced from different locations presents a cost effective alternative for producing high quality zeolites that

can be used for wide industrial and household applications. In the next phase of our study, these value added clays will be used as nanocasting agents during the synthesis of templated carbons for hydrogen storage applications. These value-addition strategies will serve to expand the existing applications of clays.

Acknowledgment

The authors would like to acknowledge National Research Foundation (NRF), Water Research Council and University of the Western Cape for support and for providing the funds to make this study possible.

References

Akbar, S., Dad, K., Shah, T. H., Shahnaz, R., 2005. Thermal studies of NaX zeolite with different degrees of cadmium exchange. *Journal of the Chemical Society of Pakistan* 27, 456-461.

Basaldella, E. I., Kikot, A., Tara, J. C., 1997. Effect of aluminum concentration on crystal size and morphology in the synthesis of a NaAl zeolite. *Materials Letters* 31, 83-86.

Barrer, R.M. (1982), "Hydrothermal Chemistry of Zeolites", Academic Press, London.

Belviso, C., Cavalcante, F., Lettino, A., Fiore, S., 2013. A and X type zeolite synthesized from kaolinite at low temperature. *Applied Clay Science* 80-81, 162-168.

Blatt, H., Middleton, G., Murray, R., 1980. *Origin of sedimentary rocks*, 2nd Edition Englewood Cliffs, N.J., Prentice-Hall, pp. 766.

Breck, D. W., 1974. *Zeolite molecular sieves*. John Wiley & Sons, New York.

Byrappa, K., Yoshimura, M. (2001), “*Handbook of Hydrothermal Technology*”, Noyes Publications / William Andrew Publishing, LLC, New York.

Coombs, D. S., Eliss, A. J., Fyfe, W. S., Taylor, A. M., 1959. The zeolite facies, with comments on their interpretation of the hydrothermal syntheses. *Geochimica Cosmochimica Acta* 17, 53-107.

Dalai, A. J, Rao, M. S., Gokhale, K. V. G. K., 1985. Synthesis of NaX zeolite using silica from rice husk ash. *Industrial & Engineering Chemistry Product Research and Development* 24, 465–468.

Donahoe, R. J., Liou, J. G., 1984. Synthesis and characterization of zeolites in the system Na₂-K₂O-Al₂O₃-SiO₂-H₂O. *Clays and Clay Minerals* 32, 433-443.

Ghosh, B., Agrawal, D.C., Bhatia, S., 1994. Synthesis of zeolite A from calcined diatomaceous clay: optimization studies. *Industrial & Engineering Chemistry Research* 33, 2107-2110.

Guggenheim, S., 1995. Definition of clay and clay mineral: Joint report of the AIPEA nomenclature and CMS nomenclature committees. *Clays and clay minerals* 43, 255-256.

Kloprogge, J. T., Komarneni, S., Amonette, J. E., 1999. Synthesis of smectite clay minerals: A critical review. *Clays and Clay Minerals* 47, 529-554.

Konta, J., 1995. Clay and man: Clay raw materials in the service of man. *Applied Clay Science* 10, 275-335.

Martinez, C., Perez-Pariente, J. (2011), "Zeolites and ordered porous solids. In: 3rd FEZA School on Zeolites : fundamentals and applications", Valencia, Editorial Universitat Politecnica de Valencia, ISBN 978-84-8363-719-7.

Mignoni, M. L., Petkowicz, D. I., Machado, N. F., Pergher, S. B. C., 2007. Synthesis of mordenite using kaolin as Si and Al source, *Applied Clay Science*, 2008, 41, 99-104.

Moisés, M. P., Pereira da Silva, C. T., Meneguim, J. G., Giroto, E M., Radovanovic, E., 2013. Synthesis of zeolite NaA from sugarcane bagasse ash. *Materials Letters* 108, 243-246.

Mollah, M. Y. A., Promreuk, S., Schennach, R., Cocke, D. L., Güler, R., 1999. Cristobalite formation from thermal treatment of Texas lignite fly ash. *Fuel* 78, 1277-1282.

Murray, H., 2000. Traditional and new applications for kaolin, smectite, and palygorskite: a general overview. *Applied Clay Science*, 17, 207–221.

Musyoka, N. M., Petrik, L. F., Fatoba, O. O., Hums, E., 2013. Synthesis of zeolites from coal fly ash using mine waters. *Minerals Engineering*, 53, 9-15.

Nagy, J. B., Bodart, P., Hannus, I., Kiricsi, I. (1998), “Synthesis, Characterization and Use of Zeolitic Microporous Materials”, Deca Gen Ltd, Szeged, Hungary.

Pfenninger, A., 1999. Molecular Sieve, Science and Technology, H.G. Karge and J. Weitkamp (Eds.), Springer-Verlag, Berlin, Vol. 2, pp. 162.

Ralph, E. G., 1968. Clay mineralogy, McGraw Hill Book Co, New York.

Schroeder, P. A., 2002. Infrared spectroscopy in clay science, CMS Workshop Lectures, Vol. 11, Teaching Clay Science, A. Rule and S. Guggenheim, eds., The Clay Mineral Society, Aurora, CO, 181-206.

Sharma, S. K., Sami, S. S., 2010. Conversion of low-grade clays to zeolite NaA. *The IUP Journal of Chemistry* 3, 32-41.

Tazaki, T., Fyfe, W. S., Van der Gaast, S. J., 1989. Growth of clay minerals in natural and synthetic glasses. *Clays & Clay Minerals* 37, 348-354.

Weitkamp, J., Puppe, L., 1999. *Catalysis and zeolites: fundamentals and application*. Springer, New York.

List of Figures

Figure 1: XRD patterns and their respective SEM micrographs for as-received bentonite, red and white clay.

Figure 2: FTIR spectra of as-received bentonite, red and white clay (before zeolitization).

Figure 3: XRD patterns and their respective SEM micrographs for zeolitization products starting from bentonite, red and white clay (without additional Al).

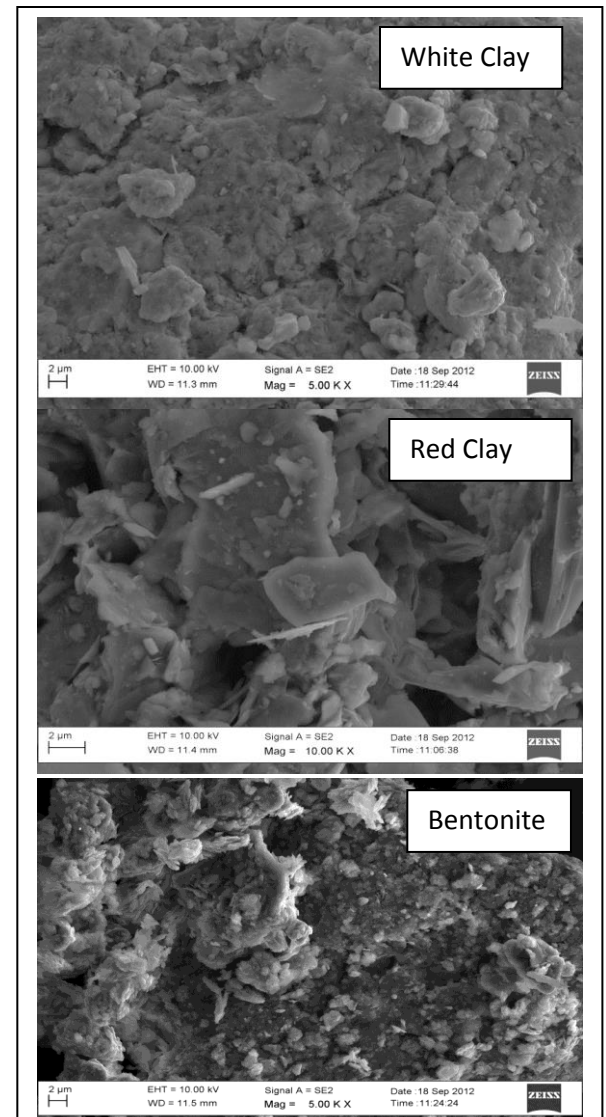
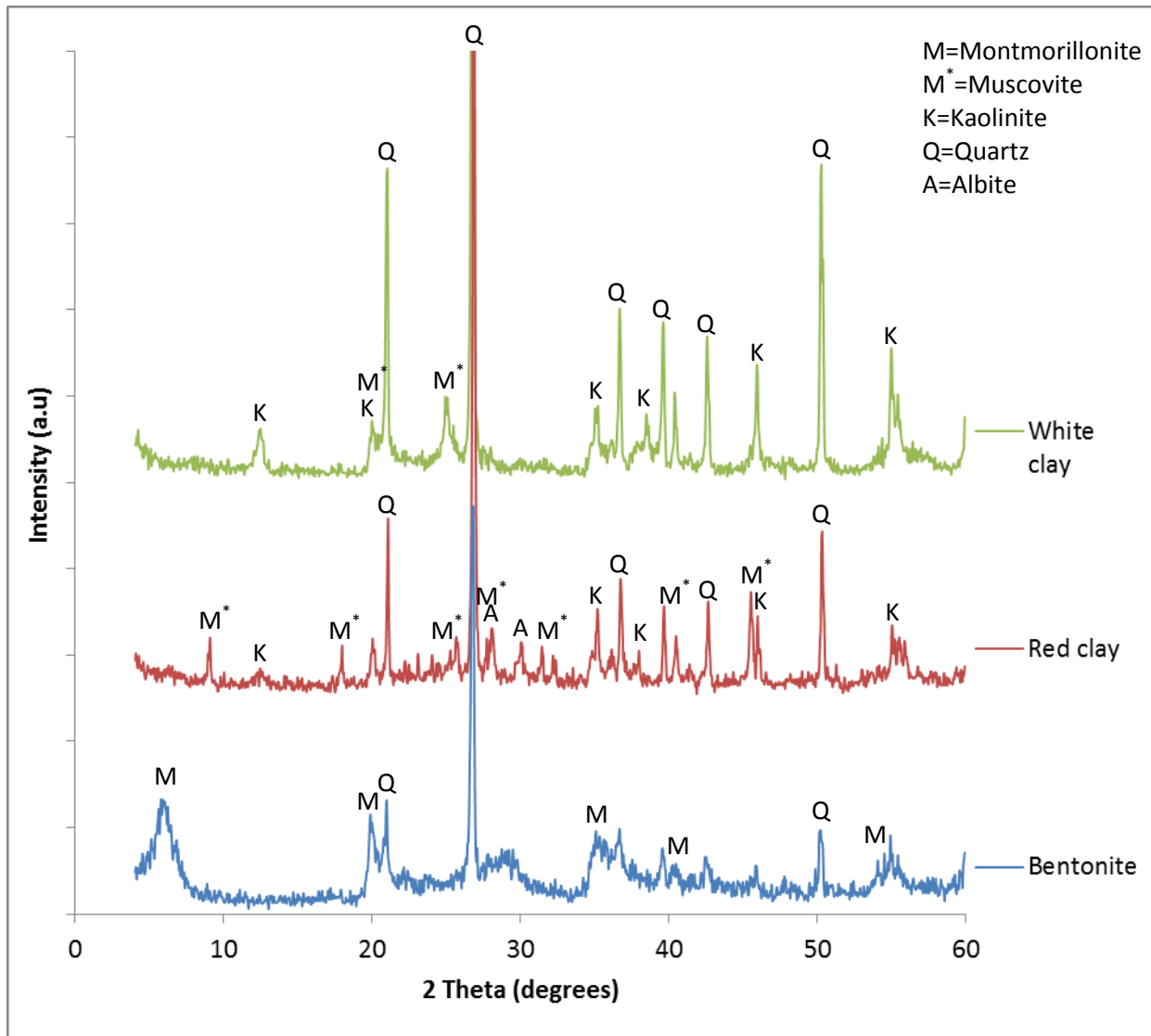
Figure 4: XRD patterns and their respective SEM micrographs for clay zeolitization products (with additional Al).

Figure 5: FTIR spectra of zeolitised bentonite, red and white clay without (a) and with (b) additional Al.

List of Tables

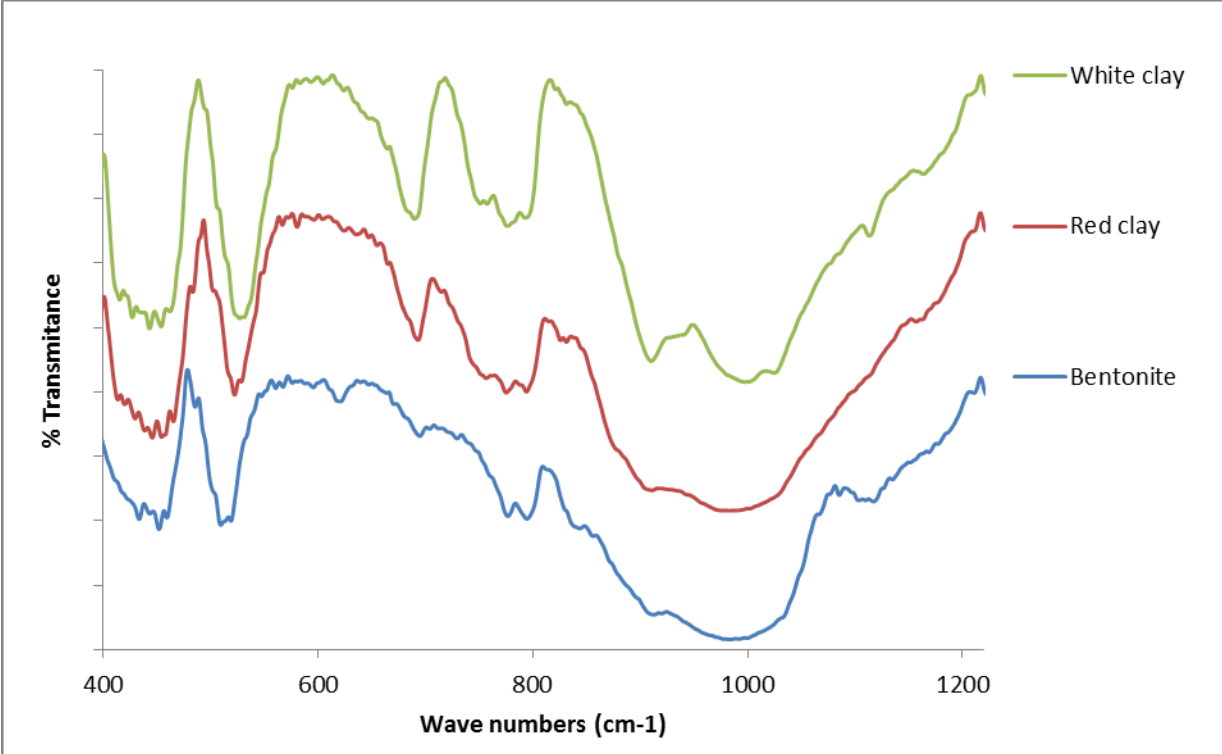
Table 1: Molar regime of unseparated fused clay slurries.

Table 2: Elemental composition of clay minerals as given by XRF analysis.



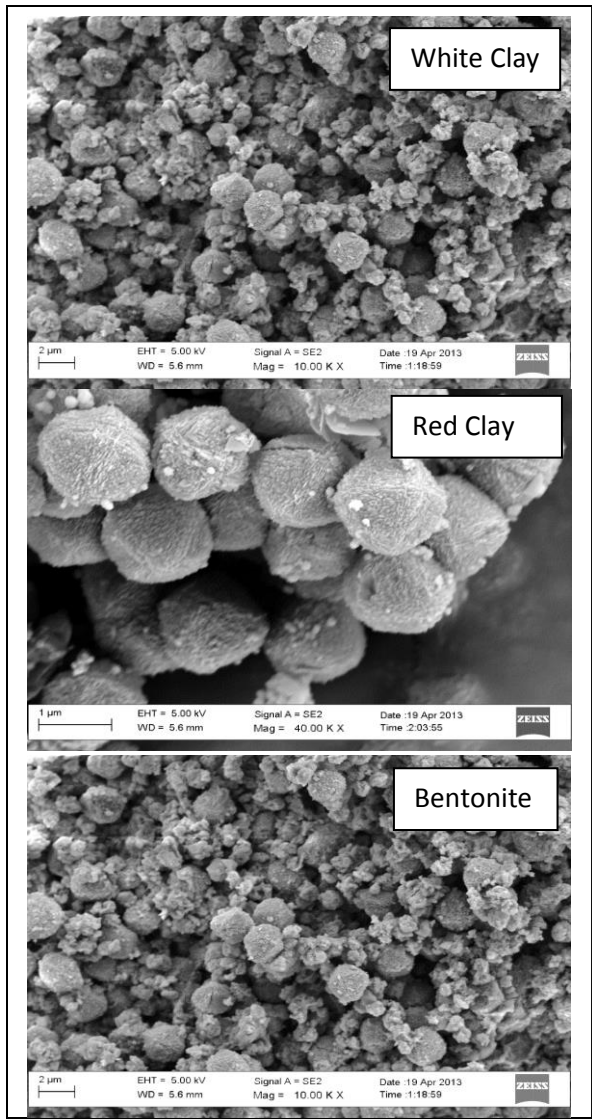
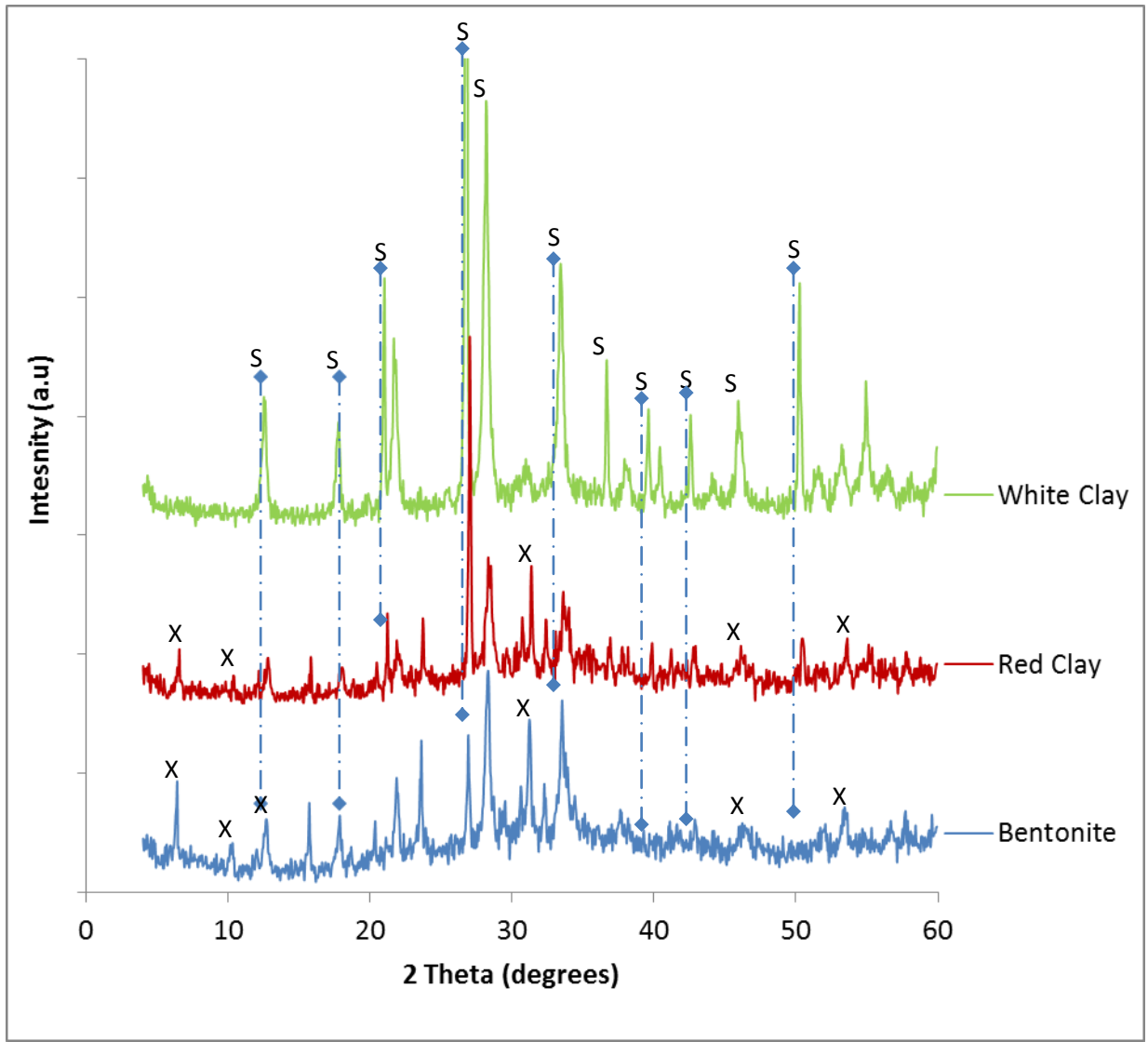
1

2 Figure 1:



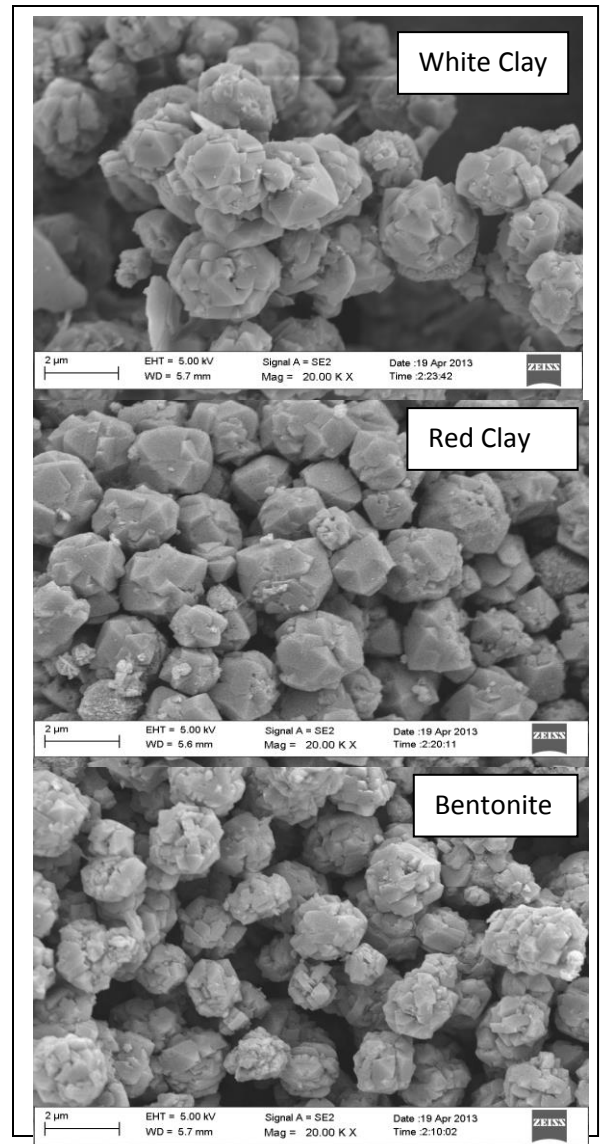
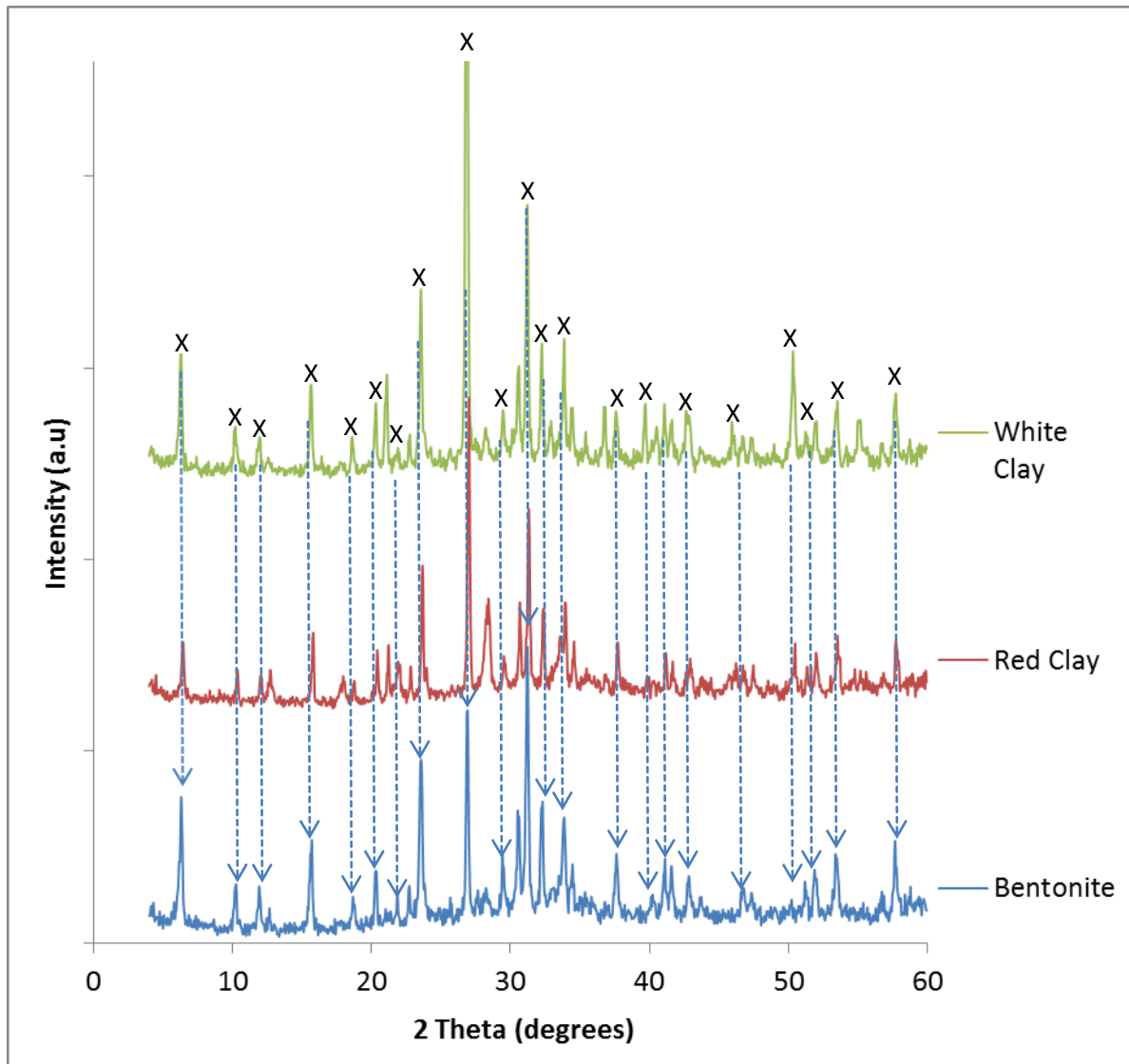
3

4 Figure 2:



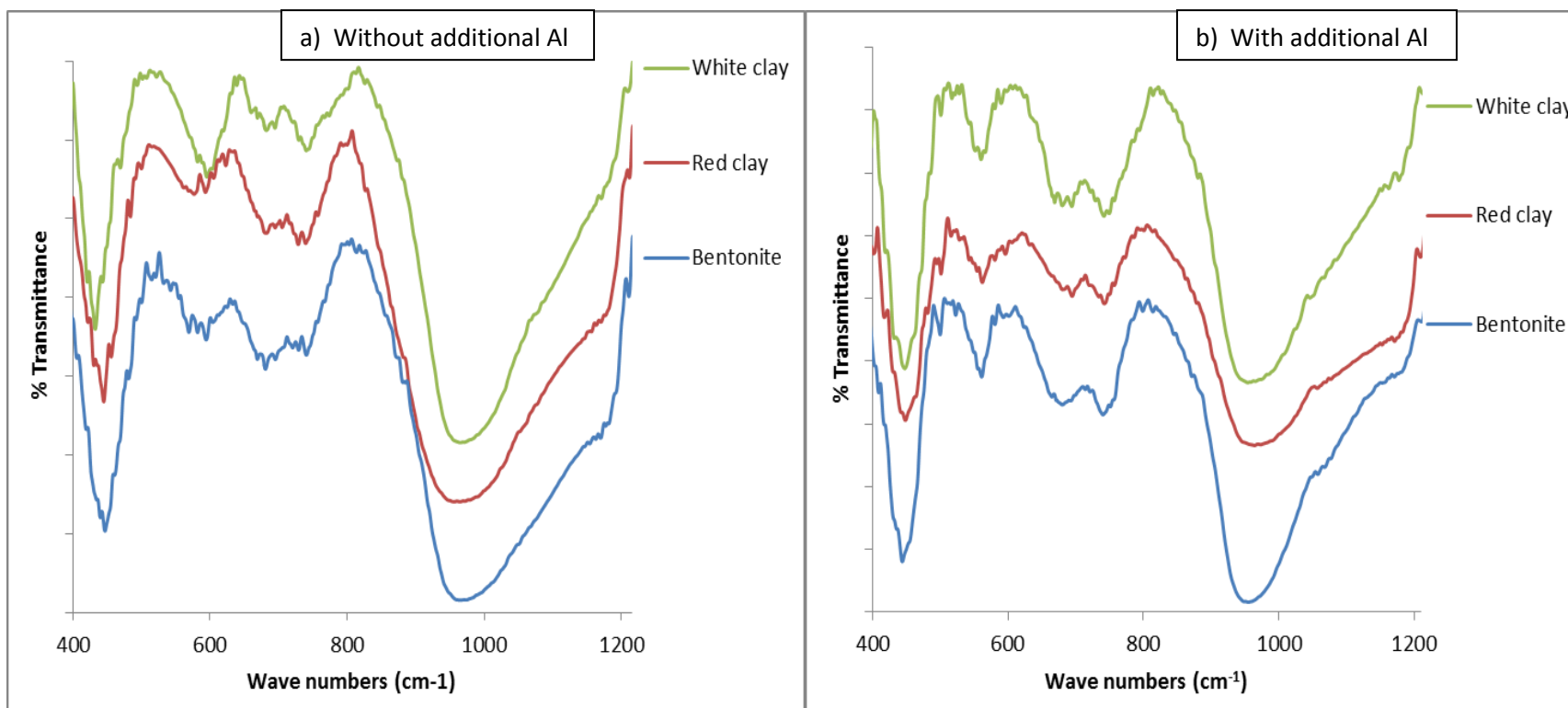
5

6 Figure 3:



7

8 Figure 4:



9

10 Figure 5:

11

12

13

14

15

16 Table 1

17 a) Without addition of $\text{Al}(\text{OH})_3$.

Bentonite	1 Al_2O_3 : 11.73 Na_2O : 7.767 SiO_2 : 480.31 H_2O
White clay	1 Al_2O_3 : 9.691 Na_2O : 7.786 SiO_2 : 403.20 H_2O
Red clay	1 Al_2O_3 : 9.868 Na_2O : 6.5477 SiO_2 : 407.32 H_2O

18

19 b) With addition of $\text{Al}(\text{OH})_3$.

Bentonite	1 Al_2O_3 : 6.271 Na_2O : 5.038 SiO_2 : 261.97 H_2O
White clay	1 Al_2O_3 : 7.110 Na_2O : 4.708 SiO_2 : 292.35 H_2O
Red clay	1 Al_2O_3 : 6.363 Na_2O : 4.222 SiO_2 : 263.70 H_2O

20

21 Table 2:

Major elements (oxide form)	Clay materials (%)		
	Bentonite	White clay	Red clay
Al₂O₃	13.29±0.02	15.80±0.06	15.62±0.08
CaO	1.03±0.00	0.03±0.01	0.89±0.00
Cr₂O₃	BD	BD	0.12±0.00
Fe₂O₃	2.64±0.01	1.22±0.01	6.12±0.01
K₂O	0.88±0.01	1.38±0.01	2.63±0.01
MgO	2.32±0.02	0.35±0.00	1.49±0.01
MnO	0.06±0.01	0.02±0.01	0.04±0.00
Na₂O	1.68±0.02	0.22±0.01	0.95±0.01
P₂O₅	0.05±0.01	0.05±0.00	0.11±0.01
SiO₂	60.80±0.08	72.56±0.14	60.25±0.15
TiO₂	0.31±0.01	1.28±0.00	0.73±0.00
LOI	17.01±0.00	6.29±0.00	10.08±0.00
Sum of conc.	100.07±0.05	99.20±0.06	99.03±0.19

22

*BD = below detection; LOI = loss on ignition